



1 **Impact of temperature dependence on the possible contribution of organics to new**  
2 **particle formation in the atmosphere**

3 Fangqun Yu<sup>1</sup>, Gan Luo<sup>1</sup>, Alexey B. Nadykto<sup>1, 2</sup>, and Jason Herb<sup>1</sup>

4

5

6 <sup>1</sup>Atmospheric Sciences Research Center, State University of New York, 251 Fuller Road,  
7 Albany, New York 12203, USA

8 <sup>2</sup>Department of Applied Mathematics, Moscow State University of Technology “Stankin”,  
9 Vadkovsky 1, Moscow, Russia

10

11

12



13 **Abstract.** Secondary particles formed via new particle formation (NPF) dominate cloud  
14 condensation nuclei (CCN) abundance in most parts of the troposphere and are important for  
15 aerosol indirect radiative forcing (IRF). Laboratory measurements have shown that certain  
16 organic compounds can significantly enhance binary nucleation of sulfuric acid and H<sub>2</sub>O.  
17 According to our recent study comparing particle size distributions measured in nine forest areas  
18 in North America with those predicted by a global size-resolved aerosol model, current H<sub>2</sub>SO<sub>4</sub>-  
19 Organics nucleation parameterizations appear to significantly over-predict NPF and particle  
20 number concentrations in summer. The lack of the temperature dependence in the current H<sub>2</sub>SO<sub>4</sub>-  
21 Organics nucleation parameterization has been suggested to be a possible reason for the observed  
22 over-prediction. In this work, H<sub>2</sub>SO<sub>4</sub>-Organics clustering thermodynamics from quantum-  
23 chemical studies has been employed to develop a scheme to incorporate temperature dependence  
24 into H<sub>2</sub>SO<sub>4</sub>-Organics nucleation parameterization. We show that temperature has a strong impact  
25 on H<sub>2</sub>SO<sub>4</sub>-Organics nucleation rates, and may reduce nucleation rate by ~ one order of  
26 magnitude per 10 K of the temperature increase. The particle number concentrations in summer  
27 over North America based on the revised scheme is a factor of more than two lower, in much  
28 better agreement with the observations. With the temperature-dependent H<sub>2</sub>SO<sub>4</sub>-Organics  
29 nucleation parameterization, the summer month CCN concentrations in the lower troposphere in  
30 the northern hemisphere are about 10-30% lower and the aerosol first IRF about 0.5 – 1.0 W/m<sup>2</sup>  
31 less negative compared to the temperature independent one. This study highlights the importance  
32 of the temperature effect and its impacts on NPF in global modeling of aerosol IRF.

33



## 34 1. Introduction

35 Atmospheric particles, through acting as cloud condensation nuclei (CCN), modify cloud  
36 properties and precipitation and thus, indirectly, affect the hydrological cycle and climate.  
37 Aerosol indirect radiative forcing (IRF) remains a major uncertainty in assessing climate change  
38 (IPCC, 2013). Secondary particles formed via nucleation dominate particle number  
39 concentrations in many parts of troposphere (Spracklen et al., 2008; Pierce and Adams, 2009; Yu  
40 and Luo, 2009), and global simulations indicate that nucleation schemes/parameterizations have  
41 a strong effect on the aerosol IRF estimations (Wang and Penner, 2009; Kazil et al., 2010; Yu et  
42 al., 2012). Different nucleation schemes, with nucleation rates depending on different variables,  
43 predict significantly different spatial patterns and seasonal variations of nucleation rates and  
44 CCN concentrations (Yu et al., 2010, 2015). Therefore, it is important to understand mechanisms  
45 of new particle formation (NPF) and the key parameters controlling the contribution of the NPF  
46 to CCN formation under wide range of varying atmospheric conditions and to validate their  
47 representation in regional and global climate models.

48 A number of laboratory chamber studies indicate that certain organic species can  
49 significantly enhance NPF (e.g., Zhang et al., 2004; Riccobono et al., 2014). This finding may  
50 have important implications for the interactions of anthropogenic and biogenic emissions and the  
51 associated climate forcing. To this regard, it is necessary to assess the ability of organics-  
52 enhanced nucleation to explain nucleation phenomena observed in the atmosphere and to  
53 determine the contribution of organics to atmospheric NPF and climate implications. In several  
54 laboratory studies, empirical parameterization of formation rate as a function of the  
55 concentrations of sulfuric acid and low-volatility highly oxidized organics has been derived  
56 (Metzger et al., 2010; Riccobono et al., 2014). One of the most important limitations of these



57 empirical parameterizations is that they were derived from the chamber measurements carried  
58 out under limited range of well-controlled conditions and, thus, reliably extrapolating these data  
59 to a wide range of atmospheric conditions remains a major issue. It should also be noted that  
60 empirical activation and kinetic nucleation formulas ( $J = k_1[\text{H}_2\text{SO}_4]$  or  $J = k_2[\text{H}_2\text{SO}_4]^2$ ) derived  
61 from limited field measurements (e.g., Riipinen et al., 2007; Kuang et al., 2008) also do not  
62 account for the impact of temperature variations on computed nucleation rates. Although these  
63 simple empirical temperature independent nucleation parameterizations have been widely used in  
64 global aerosol modeling and aerosol IRF studies (e.g., Spracklen et al., 2008; Wang and Penner,  
65 2009; Kazil et al., 2010; Scott et al., 2014; Westervelt et al., 2014; Lupascu et al., 2015), possible  
66 impacts of temperature variations were not considered in these studies.

67 In the recent study comparing particle size distributions measured in nine forest areas in  
68 North America with those predicted by a global size-resolved (sectional) aerosol model, Yu et al.  
69 (2015) showed that  $\text{H}_2\text{SO}_4$ -Organics nucleation parameterization of Riccobono et al. (2014)  
70 significantly over-predict NPF and particle number concentrations in summer (Yu et al., 2005).  
71 The lack of temperature dependence in the  $\text{H}_2\text{SO}_4$ -Organics nucleation parameterization has  
72 been suggested as a possible reason for the observed over-prediction. The main objectives of the  
73 present study are (1) to develop a scheme to incorporate temperature dependence into  $\text{H}_2\text{SO}_4$ -  
74 Organics nucleation parameterization, (2) to assess the ability of the modified parameterization  
75 in explaining the seasonal variations of NPF in NA, and (3) to study the global implications.

76

## 77 2. Methods

### 78 2.1. Organics-mediated nucleation parameterization with temperature dependence (Nucl-OrgT)



79 Based on the CLOUD chamber study of nucleation process involving sulfuric acid and  
80 organic compounds of relatively low volatility from the oxidation of pinanediol, Riccobono et al.  
81 (2014) derived the following organics-mediated nucleation parameterization (Nucl-Org),

$$82 \quad J_{\text{Nucl-Org}} = k_m \times [\text{H}_2\text{SO}_4]^2 \times [\text{BioOxOrg}] \quad (1)$$

83 where  $J_{\text{Nucl-Org}}$  is the formation rate ( $\# \text{ cm}^{-3} \text{ s}^{-1}$ ) of particles of  $\sim 1.7 \text{ nm}$ ,  $k_m$  is the fitting pre-factor  
84 with a value of  $3.27 \times 10^{-21} \text{ cm}^6 \text{ s}^{-1}$  (90% confidence interval:  $1.73 \times 10^{-21}$  to  $6.15 \times 10^{-21} \text{ cm}^6 \text{ s}^{-1}$ ),  
85  $[\text{H}_2\text{SO}_4]$  and  $[\text{BioOxOrg}]$  are the gas-phase concentrations ( $\# \text{ cm}^{-3}$ ) of  $\text{H}_2\text{SO}_4$  and biogenic  
86 oxidized organic (BioOxOrg) vapors, respectively. In the chamber study reported in Riccobono  
87 et al. (2014), BioOxOrg molecules are organic compounds of relatively low volatility from the  
88 oxidation of pinanediol (a first-generation oxidation product of  $\alpha$ -pinene) and represent later-  
89 generation oxidation products of biogenic monoterpenes.

90 The Nucl-Org parameterization given in Eq. 1, derived from laboratory chamber studies at  
91  $T=278 \text{ K}$  and  $\text{RH}=39\%$  (Riccobono et al., 2014), does not consider the possible effect of  
92 temperature on nucleation rate. According to the nucleation theory, nucleation rates are  
93 temperature-dependent unless nucleation is barrierless and limited by collision rates only.  
94 However, the value of the pre-factor  $k_m$  of  $3.27 \times 10^{-21} \text{ cm}^6 \text{ s}^{-1}$  is much smaller than well below  
95 the three-body collision rate corresponding to the formation of a cluster containing two  $\text{H}_2\text{SO}_4$   
96 and one BioOxOrg molecules. This indicates that nucleation in the CLOUD chamber under  
97 conditions reported in Riccobono et al. (2014) was not barrierless, and, thus, nucleation rates  
98 should be temperature-dependent.

99 Based on the classical homogeneous nucleation theory, the rate of nucleation ( $J$ ) can be  
100 generally written in the form

$$101 \quad J = C_1 \exp(-\Delta G/kT) \quad (2)$$



102 where  $\Delta G$  is the Gibbs free energy needed to form the critical cluster and  $C_1$  is the pre-factor.

103 With  $\Delta G = \Delta H - T \Delta S$ , where  $\Delta H$  and  $\Delta S$  are associated enthalpy and entropy change, we get

$$104 \quad J = C_1 \exp(-\Delta H/kT + \Delta S/k) = C_1 \exp(\Delta S/k) \exp(-\Delta H/kT) = C_2 \exp(-\Delta H/kT) \quad (3)$$

105 The temperature dependence of nucleation rate is dominated by the exponential term in Eq.

106 (3), although  $C_2$  may also weakly depend on temperature. Assuming that  $C_2$  is independent of

107 temperature and using  $J_{\text{Nucl-Org}}$  given in Eq. (1) as the nucleation rate at the reference temperature

108  $T_0=278$  K, we obtain

$$109 \quad J_{\text{Nucl-Org}T} = J_{\text{Nucl-Org}} f_T \quad (4)$$

$$110 \quad f_T = \exp\left[\frac{\Delta H}{k} \left(\frac{1}{T} - \frac{1}{T_0}\right)\right] \quad (5)$$

111 where  $f_T$  is the correction factor accounting for the temperature dependence.

112 One challenge here is to obtain enthalpy change ( $\Delta H$ ) associated with the critical cluster

113 formation because it is quite difficult to determine the chemical identities of BioOxOrg

114 molecules involved in atmospheric nucleation (Elm et al, 2014; Riccobono et al., 2014). As a

115 first order approximation, we use 2-Methyl-5-[(1S,2S,3R)-1,2,3,4-tetrahydroxybutyl]-3-furoic

116 acid, a select highly oxidized organic  $C_{10}H_{14}O_7$  compound, as a proxy for BioOxOrg molecules.

117 The stability of the cluster composed of two  $H_2SO_4$  and one  $C_{10}H_{14}O_7$  molecules has been

118 investigated using the Density Functional theory (DFT) at PW91PW91/6-311++G(3df,3pd) level.

119 The PW91PW91 is the most common density functional used in atmospheric studies that

120 predicts structure, vibrational spectrums, dipolar properties and thermodynamics of atmospheric

121 molecules and molecular clusters with high degree of confidence and its predictions, which have

122 been systematically validated against experimental and higher level ab initio Gibbs free energies,

123 are in a very good agreement with them for a number of atmospherically relevant molecules and



124 clusters (e.g. Herb et al., 2013, Elm et al., 2013, Nadykto et al., 2015; DePalma et al., 2015).

125 Computations have been carried out using the Gaussian 09 suite of programs (Frish et al., 2009).

126 Figure 1 presents the equilibrium geometry of the most stable isomers of heteromolecular  
127 trimer composed of  $(C_{10}H_{14}O_7)(H_2SO_4)_2$  and Table 1 reports the corresponding the  
128 thermodynamic data associated the formation of this cluster. The computational methodology,  
129 benchmarks of Gibbs free energy changes and Cartesian geometries of global minima and local  
130 minima located within  $1 \text{ kcal mol}^{-1}$  of the global minima, along with interactions of  $C_{10}H_{14}O_7$   
131 and  $H_2SO_4$  with some base molecules, will be detailed in a separate manuscript. Here, as a first  
132 order of approximation, we use  $\Delta H$  value of  $-38.30 \text{ kcal mol}^{-1}$  to calculate the temperature-  
133 dependent factor  $f_T$  in Eq. (5). Figure 2 shows the calculated value of  $f_T$  as a function of T. It is  
134 clear from Fig. 2 that  $f_T$  decreases significantly as T increases, roughly one order of magnitude  
135 per 10 K. When  $T < 269 \text{ K}$ ,  $f_T$  becomes larger than 10. In the present study,  $f_T$  is set to have a  
136 maximum value of 10. Compared to the original  $J_{\text{Nucl-Org}}$  parameterization of Riccobono et al.  
137 (2014) (Eq. 1) derived from laboratory chamber studies at  $T=278 \text{ K}$  and not taking into account  
138 the temperature dependence of nucleation rates (i.e.,  $f_T=1$ , dashed line in Fig. 2), the revised  
139 parameterization  $J_{\text{Nucl-OrgT}} = f_T J_{\text{Nucl-Org}}$  predicts quite different nucleation rate in the atmosphere,  
140 especially in the summer season, when both T and VOC emissions are at peak values.

141 It should be noted that  $f_T$  shown in Fig. 2 is subject to large uncertainty because of the  
142 potential difference between the molecules involved in the nucleation and the proxy molecule  
143 shown in Figure 1. The thermodynamic data for the formation of  $(H_2SO_4)_2(\text{BioOxOrg})$  clusters is  
144 quite limited. Elm et al. (2014) investigated the molecular interactions between the  $\alpha$ -pinene  
145 oxidation product pinic acid and sulfuric acid using computational methods and reported a  $\Delta H$   
146 value of  $-42.5 \text{ kcal/mol}$  for the formation of  $(H_2SO_4)_2(\text{Pinic Acid})$ . More negative  $\Delta H$  implies



147 stronger temperature dependence. The sensitivity of  $f_T$  values to  $\Delta H$  can be readily calculated  
148 from Eq. (4). For example, a fairly large uncertainty of  $5 \text{ kcal mol}^{-1}$  in  $\Delta H$  leads to the  
149 uncertainty in  $f_T$  of a factor of  $\sim 1.4$  at  $T=288 \text{ K}$ , while the extremely large  $20 \text{ kcal mol}^{-1}$   
150 variation in  $\Delta H$  alters  $f_T$  at  $T=288 \text{ K}$  by a factor of  $\sim 3.5$ . Despite possible uncertainties in  $f_T$ ,  
151 the temperature dependent  $J_{\text{Nucl-OrgT}}$  is likely to be more realistic than  $J_{\text{Nucl-Org}}$ , in which the  
152 temperature dependence is neglected.

153

## 154 2.2. GEOS-Chem model and global simulations

155 This work represents the first global modeling attempt in studying the effect of temperature  
156 on organics-mediated nucleation in the atmosphere. This study is built upon the work reported in  
157 Yu et al. (2015) and, thus, we use the same global model (GEOS-Chem) and configurations as  
158 that described in Yu et al. (2015). GEOS-Chem is a global 3-D model of atmospheric  
159 composition driven by assimilated meteorological observations from the Goddard Earth  
160 Observing System (GEOS) of the NASA Global Modeling and Assimilation Office (GMAO)  
161 (e.g., Bey et al., 2001). More detailed information about GEOS-Chem and updates can be found  
162 at the model website (<http://geos-chem.org/>). The aerosol simulation is based on a size-resolved  
163 (sectional) advanced particle microphysics (APM) model incorporated into GESO-Chem by Yu  
164 and Luo (2009) and considers the successive oxidation aging of the oxidation products of various  
165 VOCs (Yu, 2011). In GEOS-Chem v8-03-02, on which this study and previous work (Yu et al.,  
166 2015) are based, the concentration of highly oxidized low volatile secondary organic gas from  
167 the oxidation products of  $\alpha$ -pinenes (LV-SOG $_{\alpha\text{-pinene}}$ ) is explicitly simulated and used in Eqs. (1)  
168 and (4) to calculate organics-mediated nucleation rates. The horizontal resolution of GEOS-  
169 Chem employed in this study is  $2^\circ \times 2.5^\circ$  and there are 47 vertical model layers (with 14 layers





170 from surface to ~ 2 km above the surface). Other relevant model configurations (including  
171 emission inventories and various schemes) can be found in Yu et al. (2015).

172 The main difference between the present study and the previous one reported by Yu et al.  
173 (2015) is that the present study employs the T-dependent Nucl-Org parameterization given in Eq.  
174 (4) instead of T-independent parameterization of Riccobono et al. (2014). In addition, study of  
175 Yu et al. (2015) focuses only on the NA region, while in this work, the discussion on organics-  
176 mediated nucleation is expanded to the whole globe.

177

### 178 3. Results

179 Figure 3 shows the effect of T-dependent correction factor on simulated global distributions  
180 of monthly mean (July, 2006) nucleation rates, particle number and CCN concentrations in the  
181 boundary layer (0-1 km above the surface). The high biogenic VOC emissions in the summer  
182 coupled with strong photochemistry lead to higher concentrations of LV-SOG<sub>α-pinene</sub> or  
183 BioOxOrg (Yu et al., 2015) and hence, according to the parameterization of Riccobono et al.  
184 (2014) (i.e., Eq. 1), significant organics-mediated nucleation (Fig. 3a) and higher particle number  
185 concentrations (Figs. 3c and 3e). However, the high temperature in the summer substantially  
186 lower nucleation rates (Fig. 3b), and reduce the global monthly mean nucleation rate in the  
187 boundary layer from  $0.17 \text{ cm}^{-3}\text{s}^{-1}$  (Fig. 3a) to  $0.02 \text{ cm}^{-3}\text{s}^{-1}$ , with stronger effect in the northern  
188 hemisphere (Fig. 3b). As a result, the global monthly mean CN10 and CCN0.4 in the boundary  
189 layer decrease by 40% and 30%, respectively.

190 As we have pointed out earlier, the previous comparisons of simulated and observed particle  
191 size distributions measured in nine forest areas in North America (NA) (Yu et al., 2005) showed  
192 that  $J_{\text{Nucl-Org}}$  parameterization (Eq. 1) over-predicts particle number concentrations at these sites



193 in summer by a factor of around two on average (Yu et al., 2005). To examine the extent, at  
194 which the revised parameterization considering T-dependence (Eq. 4) can improve the agreement  
195 of simulations with measurements, we present the monthly mean horizontal distributions of  
196 CN10 zoomed into the NA region in Fig. 4. It can be clearly seen that the simulated monthly  
197 mean CN10 values in the NA boundary layer based on  $J_{\text{Nucl-OrgT}}$  (Eq. 4) are about a factor of two  
198 lower than those based on  $J_{\text{Nucl-Org}}$  (Eq. 1), with larger difference in the lower latitude part of the  
199 domain, where T is higher. In the case, when the effect of T on Nucl-Org is taken into account,  
200 the domain-wide average CN10 value decreases from 4600 to 2200  $\#/cm^3$  and the simulated  
201 particle number concentrations at the nine forest sites (with locations marked on Fig. 4, see Yu et  
202 al. (2015) for details) agree much better with the observed values.

203 To illustrate the difference and improvement, we present in Fig. 5 a set of detailed  
204 comparisons of simulated and observed evolution of particle size distributions during two ten-  
205 day periods in March and July of 2006 in Duke Forest (Pillai et al., 2013), along with time series  
206 of the concentration of condensation nuclei (CN) between 10 and 100 nm ( $\text{CN}_{10-100}$ , integrated  
207 from PSDs), which give a good overall representation of particle nucleation and growth. The  
208 observed PSDs and simulated PSDs based on  $J_{\text{Nucl-Org}}$  has been discussed in Yu et al. (2015) and  
209 are repeated here for comparison with  $J_{\text{Nucl-OrgT}}$  scheme in order to demonstrate the impact of  
210 temperature on nucleation and particle number concentrations. Although the present work  
211 focuses on the summer month, when the largest difference between  $J_{\text{Nucl-Org}}$  prediction and  
212 observation is observed, we also show in Fig. 5 simulations for a 10-day period in March as well  
213 for the comparison purpose. NPF events observed in Duke Forest are much more frequent and  
214 concentrations of nucleation mode particles are much higher in the spring than in the summer  
215 (Figs. 5a & 5b). The temperature correction (Eq. 4) has small effect in the spring (Figs. 5c, 5e,



216 and 5g) but significantly reduces nucleation rate and particle number concentration in summer  
217 (Figs. 5d, 5e, and 5f).  $J_{\text{Nucl-Org}}$  scheme (Eq. 1) predicts strong nucleation events (Fig. 5d) and  
218 significant diurnal variations in  $\text{CN}_{10-100}$  (Fig. 5h) almost every day in the summer period that  
219 obviously contradicts to observations (Fig. 5b). The high nucleation rates in the summer based  
220 on  $J_{\text{Nucl-Org}}$  scheme can be easily explained by the much higher BioOxOrg concentrations as a  
221 result of high VOC emissions and stronger photochemistry. Nevertheless, the high T in the  
222 summer inhibits nucleation (Eq. 4) and the temperature correction factor substantially improves  
223 the agreement of the simulated evolution of PSDs (Figs. 5b, 5d, 5f) and  $\text{CN}_{10-100}$  (Fig. 5h) in with  
224 observations.

225 Figure 6 shows the ratios of the CCN concentration in the lower troposphere (0-3 km) based  
226 on Nucl-Org to the CCN concentration based on Nucl-OrgT as well as the difference of aerosol  
227 first indirect radiative forcing (FIRF) ( $\text{FIRF}_{\text{Nucl-Org}} - \text{FIRF}_{\text{Nucl-OrgT}}$ ). The CCN concentrations are  
228 calculated at a water supersaturation ratio of 0.2% (CCN0.2) from simulated PSDs and the  
229 calculation of aerosol FIRF in GEOS-Chem is based on the approach discussed in Yu et al.  
230 (2013). As a result of higher nucleation rates, CCN0.2 based on Nucl-Org are about 10-20%  
231 higher than those based on Nucl-OrgT in July over most parts of northern hemisphere (Fig. 6a),  
232 with the largest difference up to 30-70% reached over part of NA, Europe, and Asia. Higher  
233 CCN leads to higher cloud droplet number concentrations and enhanced cloud albedo, resulting  
234 in an additional negative FIRF (cooling) of  $0.5 - 1.0 \text{ W/m}^2$  in a large fraction of NH with a  
235 global average of  $-0.2 \text{ W/m}^2$ .

236

237 **4. Summary and discussion**



238 Simple empirical nucleation parameterizations, which were derived from laboratory or field  
239 measurements under limited conditions and do not consider any temperature dependence of  
240 nucleation rates, have been widely used in global aerosol modeling and aerosol indirect radiative  
241 forcing studies. Based on the classical nucleation theory, temperature should be one of key  
242 parameters controlling nucleation rates, unless nucleation is barrierless. A recent study indicates  
243 (Yu et al., 2015) that the empirical parameterization of H<sub>2</sub>SO<sub>4</sub>-Organics nucleation of Riccobono  
244 et al. (2014) significantly over-predicts NPF and particle number concentrations in North  
245 America in summer. The lack of temperature dependence in the parameterization has been  
246 suggested as a likely reason for the observed over-prediction. In the present study, H<sub>2</sub>SO<sub>4</sub>-  
247 Organics clustering thermodynamics from quantum-chemical studies has been employed to  
248 develop a scheme for incorporating the temperature dependence into H<sub>2</sub>SO<sub>4</sub>-Organics nucleation  
249 parameterization, which reduces global mean nucleation rate in the boundary layer in a summer  
250 month is by a factor of ~ 8 and improves the agreement of predicted particle number  
251 concentrations over North America with observations. With temperature-dependent H<sub>2</sub>SO<sub>4</sub>-  
252 Organics nucleation parameterization, the summer month CCN concentrations in the lower  
253 troposphere in the northern hemisphere are about 10-30% lower, and the aerosol first IRF about  
254 0.5 – 1.0 W/m<sup>2</sup> less negative compared to temperature independent one. In view of the potential  
255 effects of changes in CCN concentrations on precipitation (second indirect impact) and cloud  
256 cover, it is important to reduce uncertainties in NPF calculation in regional and global climate  
257 models.

258 The study highlights the importance of including the temperature dependence of nucleation  
259 rates in global modeling of NPF and aerosol indirect radiative forcing. The temperature  
260 dependence factor derived under this study represents the first (to our knowledge) attempt of



261 studying the temperature effect on organics-mediated nucleation in the global atmosphere and  
262 improves the agreement between simulated particle number concentrations and observations in  
263 NA. Although it may subject to uncertainties due to the possible difference between the  
264 molecules involved in the nucleation and the proxy molecule, temperature dependent  $J_{\text{Nucl-OrgT}}$ ,  
265 likely more realistic than  $J_{\text{Nucl-Org}}$ , in which the temperature dependence is neglected. Further  
266 laboratory measurements and theoretical studies are needed to better understand the effect of  
267 temperature on organics-mediated nucleation in the atmosphere.

268

269 **Acknowledgments.** This study was supported by NASA under grant NNX13AK20G and US  
270 National Science Foundation (NSF) under grant 1550816. The GEOS-Chem model is managed  
271 by the Atmospheric Chemistry Modeling Group at Harvard University with support from  
272 NASA's Atmospheric Chemistry Modeling and Analysis Program.

273

## 274 **References**

275 Bey, I., Jacob, D. J., Yantosca, R. M., Logan, J. A., Field, B., Fiore, A. M., Li, Q., Liu, H.,  
276 Mickley, L. J., and Schultz, M.: Global modeling of tropospheric chemistry with assimilated  
277 meteorology: Model description and evaluation, *Journal of Geophysical Research*, 106,  
278 23,073–23,096, 2001.

279 DePalma, J. W., Wang, A. S., Wexler, and M.V Johnston, Growth of ammonium bisulfate  
280 clusters by adsorption of oxygenated organic molecules, *The Journal of Physical Chemistry*  
281 A, 119 (45), 11191–11198, DOI: 10.1021/acs.jpca.5b07744, 2015.

282 Elm, J., M. Bilde, and K. V. Mikkelsen: Assessment of binding energies of atmospherically  
283 relevant clusters. *Physical Chemistry Chemical Physics* 15.39, 16442-16445., 2013.



- 284 Elm, J., T. Kurten, M. Bilde and K.V. Mikkelsen: Molecular interaction of pinic acid with  
285 sulfuric acid: Exploring the thermodynamic landscape of cluster growth, *The Journal of*  
286 *Physical Chemistry A*, 2014, 118, 7892–7900, 2014.
- 287 Frisch, M. J.; Trucks, G. W.; Schlegel, H. B.; Scuseria, G. E.; Robb, M. A.; Cheeseman, J. R.;  
288 Scalmani, G.; Barone, V.; Mennucci, B.; et al.: Gaussian 09, Gaussian, Inc., Wallingford CT,  
289 2009.
- 290 Herb, J., Y. Xu, F. Yu, and A. B. Nadykto, Large hydrogen-bonded pre-nucleation ( $\text{HSO}_4^-$ )  
291  $(\text{H}_2\text{SO}_4)_m(\text{H}_2\text{O})_k$  and  $(\text{HSO}_4^-)(\text{NH}_3)(\text{H}_2\text{SO}_4)_m(\text{H}_2\text{O})_k$  Clusters in the Earth's Atmosphere, *The*  
292 *Journal of Physical Chemistry A*, 117 (1), 133–152, 2013.
- 293 IPCC, *Climate Change 2013: The Physical Scientific Basis*, edited by T. F. Stocker, D. Qin, et al.,  
294 Cambridge Univ. Press, New York, USA, 2013.
- 295 Kazil, J., Stier, P., Zhang, K., Quaas, J., Kinne, S., O'Donnell, D., Rast, S., Esch, M., Ferrachat,  
296 S., Lohmann, U., and Feichter, J.: Aerosol nucleation and its role for clouds and Earth's  
297 radiative forcing in the aerosol-climate model ECHAM5-HAM, *Atmospheric Chemistry and*  
298 *Physics*, 10, 10733-10752, doi:10.5194/acp-10-10733-2010, 2010.
- 299 Kuang, C., McMurry, P. H., McCormick, A. V., and Eisele, F. L.: Dependence of nucleation  
300 rates on sulfuric acid vapor concentration in diverse atmospheric locations, *J. Geophys. Res.*,  
301 113, D10209, doi:10.1029/2007JD009253, 2008.
- 302 Lupascu, A., Easter, R., Zaveri, R., Shrivastava, M., Pekour, M., Tomlinson, J., Yang, Q., Matsui,  
303 H., Hodzic, A., Zhang, Q., and Fast, J. D.: Modeling particle nucleation and growth over  
304 northern California during the 2010 CARES campaign, *Atmos. Chem. Phys.*, 15, 12283-  
305 12313, doi:10.5194/acp-15-12283-2015, 2015.



306 Metzger, A., Verheggen, B., Dommen, J., Duplissy, J., Prevot, A.S., Weingartner, E., Riipinen, I.,  
307 Kulmala, M., Spracklen, D.V., Carslaw, K.S. and Baltensperger, U.: Evidence for the role of  
308 organics in aerosol particle formation under atmospheric conditions, Proceedings of the  
309 National Academy of Sciences, 107(15), pp.6646-6651, 2010.

310 Nadykto, A. B., J. Herb, F.Yu, and Y. Xu: Enhancement in the production of nucleating clusters  
311 due to dimethylamine and large uncertainties in the thermochemistry of amine-enhanced  
312 nucleation, Chemical Physics Letters, 609, 42-49, 2015.

313 Pierce, J.R., and Adams, P.J.: Uncertainty in global CCN concentrations from uncertain aerosol  
314 nucleation and primary emission rates, Atmospheric Chemistry and Physics, 9, 1339-1356,  
315 2009.

316 Pillai, P., Khlystov, A., Walker, J. and Aneja, V. Observation and analysis of particle nucleation  
317 at a forest site in southeastern US. Atmosphere. 4(2):72-93, 2013.

318 Riccobono, FSchoberberger, S., Scott, C.E., Dommen, J., Ortega, I.K., Rondo, L., Almeida, J.,  
319 Amorim, A., Bianchi, F., Breitenlechner, M., David, A., Downard, A., Dunne, E.M.,  
320 Duplissy, J., Ehrhardt, S., Flagan, R.C., Franchin, A., Hansel, A., Juuninen, H., Kajos, M.,  
321 Keskinen, H., Kupc, A., Kürten, A., Kvashin, A.N., Laaksonen, A., Lehtipalo, K.,  
322 Makkmutov, V., Mathot, S., Nieminen, T., Onnela, A., Petäjä, T.,Praplan, A.P., Santos, F.D.,  
323 Schallhart, S., Seinfeld, J.H., Sipilä, M., Spracklen, D.V., Stozhkov, Y., Stratmann, F., Tomé,  
324 A., Tsagkogeorgas, G., Vaattlovaara, P., Viisanen, Y., Vrtala, A., Wagner, P.E., Weingartner,  
325 E., Wex, H., Wimmer, D., Carslaw, K.S., Curtius, J., Donahue, N.M., Kirkby, J., Kulmala, M.  
326 Worsnop, D.R., and Baltensperger, U.: Oxidation products of biogenic emissions contribute  
327 to nucleation of atmospheric particles, Science, 344, 717, 2014.



- 328 Riipinen, I., S.-L. Sihto, M. Kulmala, F. Arnold, M. Dal Maso, W. Birmili, K. Saarnio, K.  
329 Teinilä, V.-M. Kerminen, A. Laaksonen, and K. E. J. Lehtinen: Connections between  
330 atmospheric sulphuric acid and new particle formation during QUEST III–IV campaigns in  
331 Heidelberg and Hyytiälä, *Atmos. Chem. Phys.*, 7, 1899–1914, 2007.
- 332 Scott, C. E., Rap, A., Spracklen, D. V., Forster, P. M., Carslaw, K. S., Mann, G. W., Pringle, K.  
333 J., Kivekäs, N., Kulmala, M., Lihavainen, H., and Tunved, P.: The direct and indirect  
334 radiative effects of biogenic secondary organic aerosol, *Atmos. Chem. Phys.*, 14, 447–470,  
335 doi:10.5194/acp-14-447-2014, 2014.
- 336 Spracklen, D. V., Carslaw, K. S., Kulmala, M., Kerminen, V.-M., Sihto, Riipinen, I., Merikanto,  
337 J., Mann, G.W., Chipperfield, M.P., Wiedensohler, A., Birmili, W., and Lihavainen, H.:  
338 Contribution of particle formation to global cloud condensation nuclei concentrations,  
339 *Geophysical Research Letters*, 35, L06808, doi:10.1029/2007GL033038, 2008.
- 340 Wang, M. and Penner, J. E.: Aerosol indirect forcing in a global model with particle nucleation,  
341 *Atmospheric Chemistry and Physics*, 9, 239–260, 2009.
- 342 Westervelt, D. M., Pierce, J. R., and Adams, P. J.: Analysis of feedbacks between nucleation rate,  
343 survival probability and cloud condensation nuclei formation, *Atmos. Chem. Phys.*, 14,  
344 5577–5597, doi:10.5194/acp-14-5577-2014, 2014.
- 345 Yu, F.: A secondary organic aerosol formation model considering successive oxidation aging and  
346 kinetic condensation of organic compounds: global scale implications, *Atmospheric  
347 Chemistry and Physics*, 11, 1083–1099, doi:10.5194/acp-11-1083-2011, 2011.
- 348 Yu, F., and G. Luo: Simulation of particle size distribution with a global aerosol model:  
349 contribution of nucleation to aerosol and CCN number concentrations. *Atmospheric  
350 Chemistry and Physics*, 9, 7691–7710, 2009.





351 Yu, F., G. Luo, T. Bates, B. Anderson, A. Clarke, V. Kapustin, R. Yantosca, Y. Wang, S.  
 352 Wu: Spatial distributions of particle number concentrations in the global troposphere:  
 353 Simulations, observations, and implications for nucleation mechanisms, *J. Geophys. Res.*,  
 354 115, D17205, doi:10.1029/2009JD013473, 2010.

355 Yu, F., Luo, G., Liu, X., Easter, R. C., Ma, X., and Ghan, S. J.: Indirect radiative forcing by ion-  
 356 mediated nucleation of aerosol, *Atmospheric Chemistry and Physics*, 12, 11451-11463, 2012.

357 Yu, F., X. Ma, and G. Luo: Anthropogenic contribution to cloud condensation nuclei and the  
 358 first aerosol indirect climate effect, *Environmental Research Letters* 8 024029  
 359 doi:10.1088/1748-9326/8/2/024029, 2013.

360 Yu, F., Luo, G., Pryor, S. C., Pillai, P. R., Lee, S. H., Ortega, J., Schwab, J. J., Hallar, A. G.,  
 361 Leaitch, W. R., Aneja, V. P., Smith, J. N., Walker, J. T., Hogrefe, O., and Demerjian, K. L.:  
 362 Spring and summer contrast in new particle formation over nine forest areas in North  
 363 America, *Atmos. Chem. Phys.*, 15, 13993-14003, doi:10.5194/acp-15-13993-2015, 2015.

364 Zhang, R., I. Suh, J. Zhao, D. Zhang, E.C. Fortner, X. Tie, L.T. Molina, and M.J. Molina:  
 365 Atmospheric new particle formation enhanced by organic acids, *Science*, 304, 1487-1490,  
 366 2004.

367

368

369 Table 1. Changes of enthalpy ( $\Delta H$ ), entropy ( $\Delta S$ ), and Gibbs free energy ( $\Delta G$ ) for the formation  
 370 of  $(C_{10}H_{14}O_7)(H_2SO_4)_2$  cluster under the standard condition ( $P=1$  atm,  $T=298$  K).

	$\Delta H$ (kcal mol <sup>-1</sup> )	$\Delta S$ (cal mol <sup>-1</sup> K <sup>-1</sup> )	$\Delta G$ (kcal mol <sup>-1</sup> )
$C_{10}H_{14}O_7 + H_2SO_4 + H_2SO_4 \rightleftharpoons (C_{10}H_{14}O_7)(H_2SO_4)_2$	-38.30	-75.45	-15.81

371



372 **Figure Captions**

373 **Figure 1.** Equilibrium geometry of the most stable isomers of heteromolecular trimer composed  
374 of  $(C_{10}H_{14}O_7)(H_2SO_4)_2$  obtained at PW91PW91/6-311++G(3df,3pd) level of theory. Bonding  
375 lengths are in angstroms.

376 **Figure 2.** Calculated temperature dependence correction factor for Nucl-Org parameterization  
377 ( $f_T$ ) as a function of T.

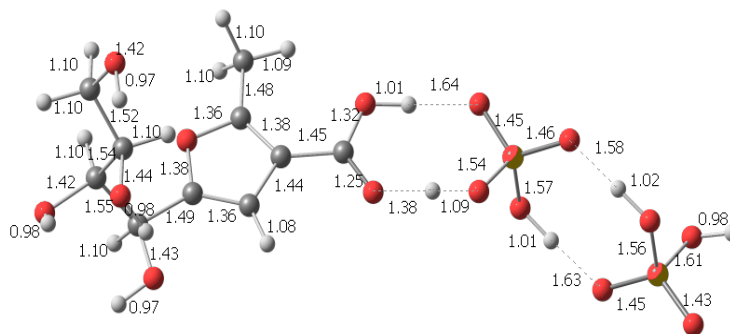
378 **Figure 3.** Horizontal distributions of monthly mean nucleation rates (J) (a, b), concentrations of  
379 condensation nuclei larger than 10 nm (CN10) (c, d), and concentrations of cloud condensation  
380 nuclei at water supersaturation ratio of 0.4% (CCN0.4) (e, f) in the boundary layer (0-1 km above  
381 the surface) in July of 2006 based on two organics-mediated nucleation schemes:  $J_{\text{Nucl-Org}}$  (left  
382 panels) and  $J_{\text{Nucl-OrgT}}$  (right panels).

383 **Figure 4.** Horizontal distributions of monthly mean CN10 in the boundary layer (0-1 km above  
384 surface) in July of 2006 based on two organics-mediated nucleation schemes: (a)  $J_{\text{Nucl-Org}}$  and (b)  
385  $J_{\text{Nucl-OrgT}}$ . The locations of 9 forest sites where observed particle size distributions measurements  
386 have been used for comparisons in Yu et al. (2015) are marked.

387 **Figure 5.** Particle size distributions (PSDs) observed (a, b) and simulated based on Nucl-Org (c,  
388 d) and Nucl-OrgT (e, f) schemes during two ten-day periods in March (a, c, e) and July (b, d, f)  
389 of 2006 in Duke Forest (DUK), along with time series of the concentration of condensation  
390 nuclei between 10 and 100 nm ( $CN_{10-100}$ ) (g, h).

391 **Figure 6.** (a) Ratios of the concentration of CCN (at water supersaturation ratio of 0.2%) in the  
392 lower troposphere (0-3 km) based on Nucl-Org scheme to those based on Nucl-OrgT scheme,  
393 and (b) Difference of aerosol first indirect radiative forcing (FIRF) ( $FIRF_{\text{Nucl-Org}} - FIRF_{\text{Nucl-OrgT}}$ ).

394

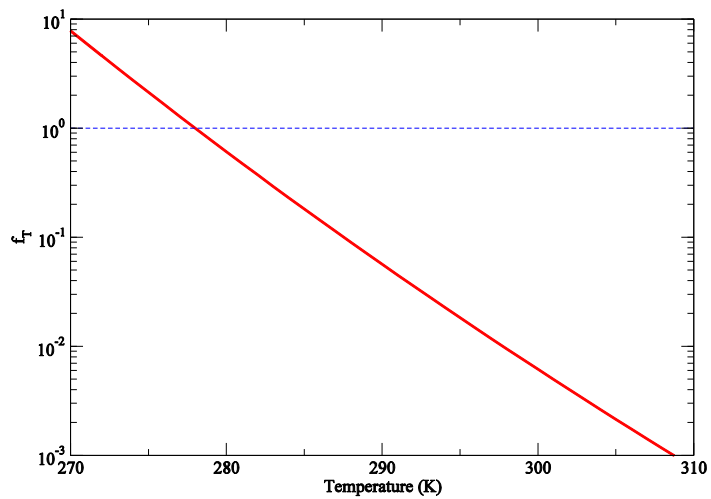


395

396 Figure 1.

397

398



399

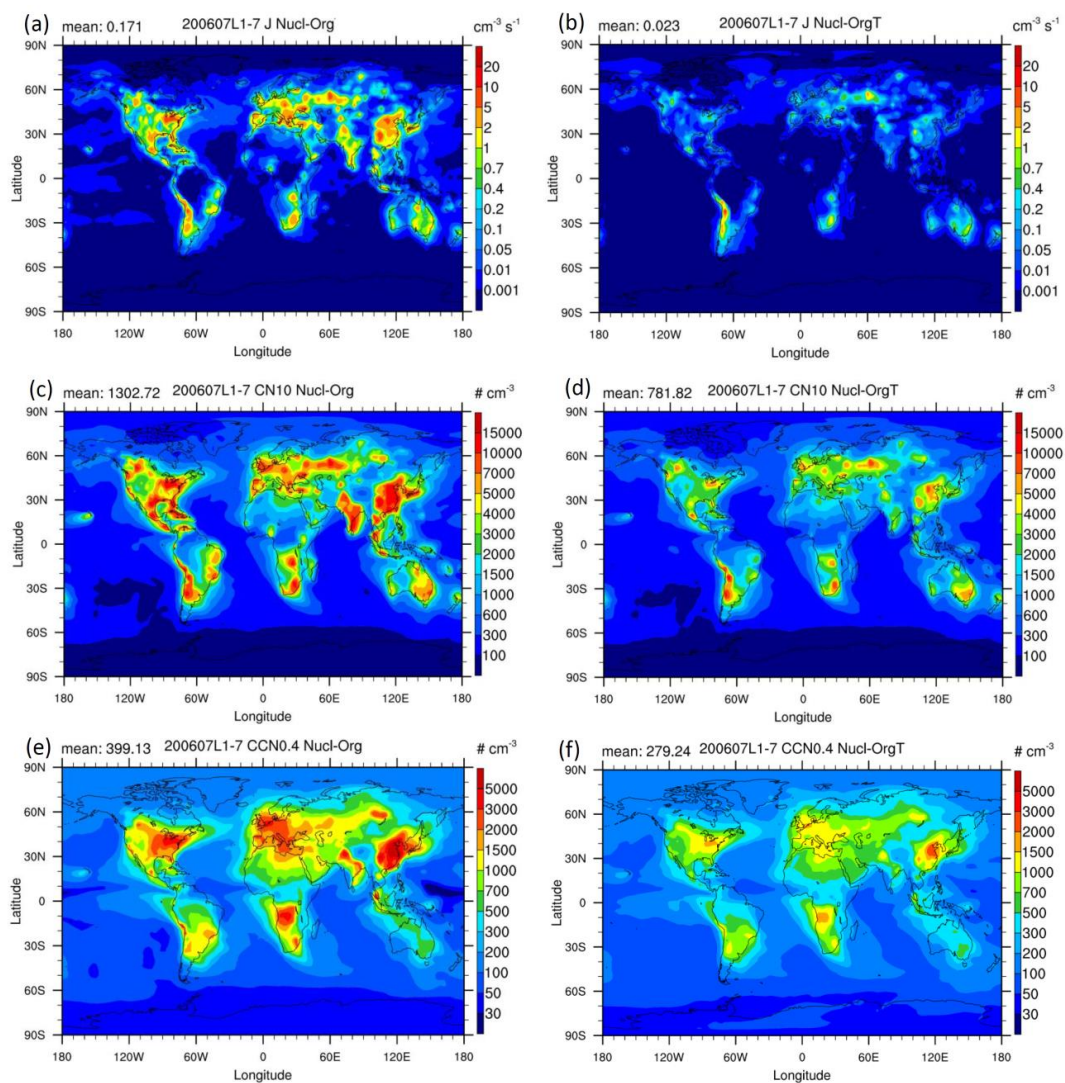
400

401 Figure 2.

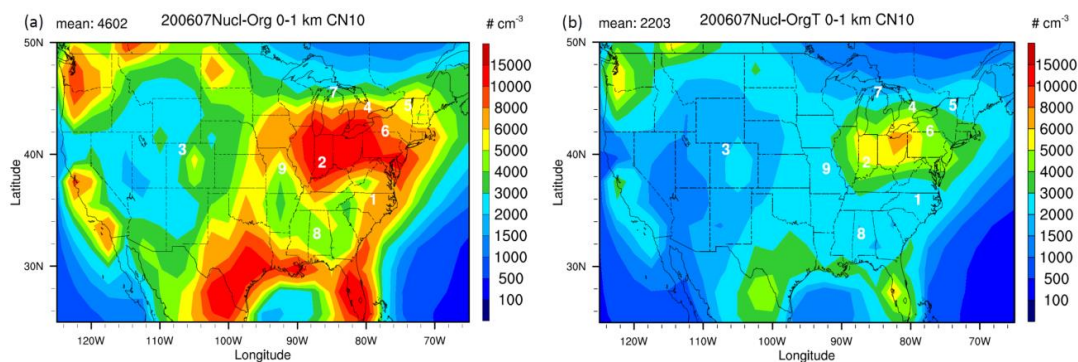
402

403

404



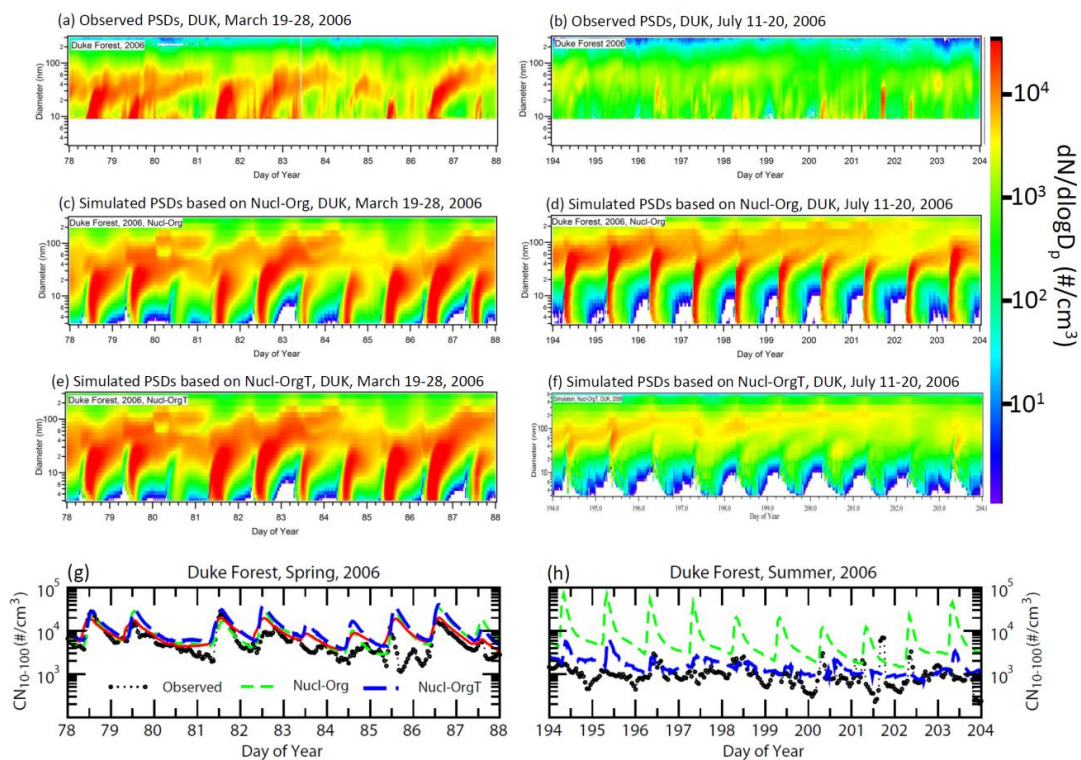
405  
406 Figure 3.  
407  
408



409  
 410 Figure 4.

411

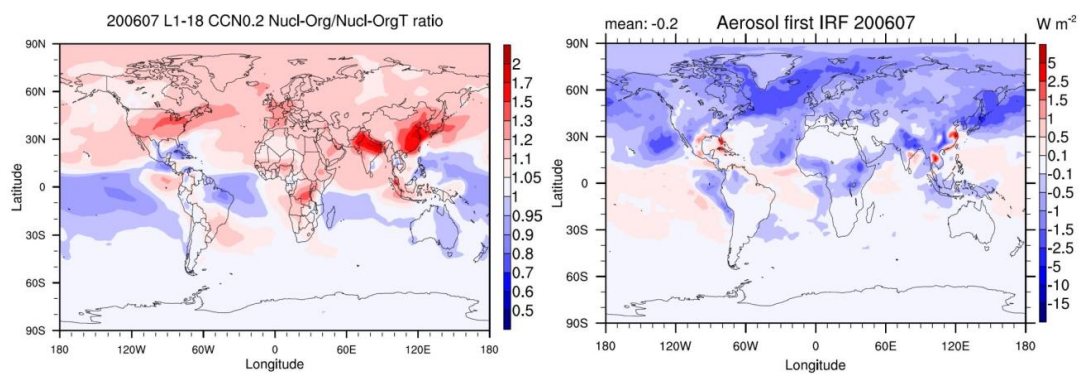
412



413  
 414 Figure 5.

415





416

417 Figure 6.

418